

Article

Hydrolytic Mechanism of a Metalloenzyme Is Modified by the Nature of the Coordinated Metal Ion

Zeyad H. Nafae^{1,2}, Bálint Hajdu¹ , Éva Hunyadi-Gulyás³  and Béla Gyurcsik^{1,*} 

¹ Department of Inorganic, Organic and Analytical Chemistry, University of Szeged, Dóm tér 7, H-6720 Szeged, Hungary; n.zeyad@chem.u-szeged.hu (Z.H.N.); balinth11@chem.u-szeged.hu (B.H.)

² College of Pharmacy, University of Babylon, Hillah 51001, Iraq

³ Laboratory of Proteomics Research, Biological Research Centre, Eötvös Loránd Research Network, Temesvári krt. 62, H-6726 Szeged, Hungary; gulyas.eva@brc.hu

* Correspondence: gyurcsik@chem.u-szeged.hu; Tel.: +36-6254-4335

Abstract: The nuclease domain of colicin E7 cleaves double-strand DNA non-specifically. Zn²⁺ ion was shown to be coordinated by the purified NCoLE7 as its native metal ion. Here, we study the structural and catalytic aspects of the interaction with Ni²⁺, Cu²⁺ and Cd²⁺ non-endogenous metal ions and the consequences of their competition with Zn²⁺ ions, using circular dichroism spectroscopy and intact protein mass spectrometry. An R447G mutant exerting decreased activity allowed for the detection of nuclease action against pUC119 plasmid DNA via agarose gel electrophoresis in the presence of comparable metal ion concentrations. It was shown that all of the added metal ions could bind to the apoprotein, resulting in a minor secondary structure change, but drastically shifting the charge distribution of the protein. Zn²⁺ ions could not be replaced by Ni²⁺, Cu²⁺ and Cd²⁺. The nuclease activity of the Ni²⁺-bound enzyme was extremely high in comparison with the other metal-bound forms, and could not be inhibited by the excess of Ni²⁺ ions. At the same time, this activity was significantly decreased in the presence of equivalent Zn²⁺, independent of the order of addition of each component of the mixture. We concluded that the Ni²⁺ ions promoted the DNA cleavage of the enzyme through a more efficient mechanism than the native Zn²⁺ ions, as they directly generate the nucleophilic OH[−] ion.

Keywords: colicin E7; metallo nuclease; circular dichroism; mass spectrometry; gel electrophoresis



Citation: Nafae, Z.H.; Hajdu, B.; Hunyadi-Gulyás, É.; Gyurcsik, B. Hydrolytic Mechanism of a Metalloenzyme Is Modified by the Nature of the Coordinated Metal Ion. *Molecules* **2023**, *28*, 5511. <https://doi.org/10.3390/molecules28145511>

Academic Editors: Gianantonio Battistuzzi and Carlo Augusto Bortolotti

Received: 6 June 2023

Revised: 11 July 2023

Accepted: 17 July 2023

Published: 19 July 2023



Copyright: © 2023 by the authors. Licensee MDPI, Basel, Switzerland. This article is an open access article distributed under the terms and conditions of the Creative Commons Attribution (CC BY) license (<https://creativecommons.org/licenses/by/4.0/>).

1. Introduction

Colicins represent a class of bacterial toxins, and as such they are intriguing targets of antibiotic research [1,2]. They are classified based on the mode of import into the attacked cells or on the mechanism of the toxicity [3,4]. Colicin E7 is a metalloprotein, produced by *Escherichia coli* under stress conditions to protect the cells from related bacteria as part of the cell defence mechanism [5,6]. Colicin E7 consists of three domains: the receptor-binding domain recognises the target cell surface, the translocation domain facilitates traffic across the cell membrane and the nuclease domain NCoLE7 is cleaved off while entering the cell, and it digests the cell's DNA non-specifically [4,6–9]. The Im7 immunity protein is co-expressed with colicin E7 in the host cell, protecting it from nuclease action by interacting with the DNA binding site of NCoLE7 [8] (Figure 1). NCoLE7 is thus expressed and purified together with the Im7 protein under laboratory conditions. The HNH active site of the NCoLE7 enzyme is located at the C-terminus and exhibits a characteristic $\beta\beta\alpha$ secondary structure. The H545 histidine side-chain is suggested to participate in the generation of the OH[−] ion nucleophile by promoting the deprotonation of the catalytic water molecule [10,11]. A divalent metal ion is bound by H544, H569 and H573 imidazole side-chains (throughout the text we apply the original numbering related to the full-size colicin E7 protein for better comparison with the literature data) in the active centre. Several crystal structures demonstrated that the metal ion can also bind a water molecule [12–14],

to a phosphate [10,12,15] or sulphate [12,16] anion or to the scissile phosphodiester bond of the substrate DNA [17,18] via the fourth binding site in the tetrahedral geometry. This binding site proved to show a high affinity for Zn^{2+} ions, which are the metal ions that can be detected in NCoIE7, as obtained from the cells [14,17,19]. Purification by immobilised Ni^{2+} ion chromatography through oligohistidine tags may result in the replacement of Zn^{2+} , while the procedure to break up the bonding between NCoIE7 and Im7 by decreasing the pH to ~ 3.0 leads to the apoprotein as the final product after separation from Im7 and renaturation [20,21].

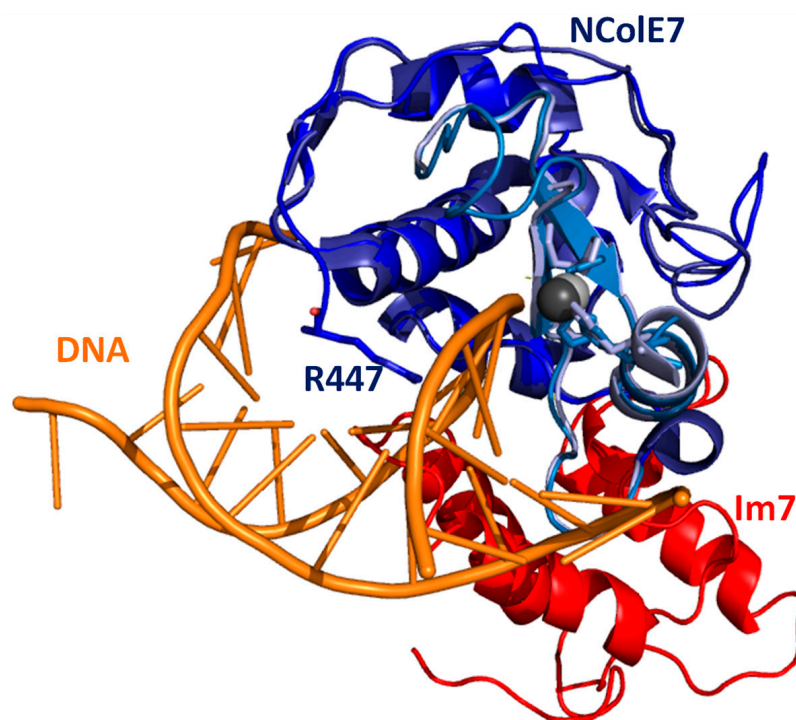


Figure 1. The X-ray structures of NCoIE7 (blue, with the HNH motif in light blue) together with Im7 protein (red, pdb ID: 7CEI [14]) and with short DNA (orange, pdb ID: 1ZNS [17]) are overlaid through their NCoIE7 parts. The figure shows the interference between the binding sites of Im7 and DNA. The three histidines bound to Zn^{2+} ion are highlighted by sticks, similarly to the R447, which is mutated in our study to G447.

Through mutational study, we have previously shown that the catalytic site of NCoIE7 is pre-organised to form the optimal tetrahedral cavity for Zn^{2+} ion binding. The 25 residue long N-terminal loop of NCoIE7 without a specific secondary structure was examined via computational modelling [22]. The suggested W464A mutation was identified to exert a dramatic effect on Zn^{2+} ion binding, as well as on the protein structure [23]. However, the structure and Zn^{2+} -affinity were restored both via Im7 and DNA binding. This also draws attention to the fact that the structures of NCoIE7 crystallised together with these interacting agents reflect the induced position, instead of the native one [24].

N-terminal amino acids, with the main emphasis on R447, have been shown to promote the catalytic activity of NCoIE7. Removing R447 decreases the catalytic activity to $\sim 10\%$ of that of NCoIE7 [19,25]. As can also be seen in the tertiary structure, the N-terminus of the protein becomes close to the catalytic site so that it may interact with the DNA substrate (Figure 1). Such a conserved arginine in the *Serratia marcescens* endonuclease family was supposed to play a role in the positioning and polarisation of the scissile phosphodiester, but may also be involved in transition-state stabilisation [26]. We have previously shown that the mutation of the R447 arginine to glycine in NCoIE7 did not significantly influence the solution structure and DNA binding property of the protein [20], but it is easier to study its catalytic activity than that of the very active NCoIE7 enzyme.

The aim of this work was to investigate the ability of the KGNK protein mutant of NCoIE7 (Scheme 1) to bind transition metal ions such as Ni²⁺, Cu²⁺ and Cd²⁺ ions in the presence and absence of Zn²⁺ [20], as well as the effect of various metal ions on the catalytic process. We expected that the non-endogenous metal ions may be applied for the fine tuning of the enzyme activity.

NCoIE7 KRNKPGKATGKPKVNNKWLNNAGKDLGSPVPDRIANKLRDKEFKSFDDFRKKFWEEVSKDPELSKQ
 KGNK GPLGSPEFK ENKPGKATGKPKVNNKWLNNAGKDLGSPVPDRIANKLRDKEFKSFDDFRKKFWEEVSKDPELSKQ

FSRNNDRMKVGKAPKTRTQDVSGKRTSFELHHEKPI SQNGGVYMDNISVVTPKRHIDIHRGK
FSRNNDRMKVGKAPKTRTQDVSGKRTSFELHHEKPI SQNGGVYMDNISVVTPKRHIDIHRGK

Scheme 1. Comparison of the amino acid sequences of the studied KGNK mutant and NCoIE7 proteins. The R447G mutation is highlighted by a red background, and the N-terminal sequence that remained after the GST cleavage is underlined. This amino acid section of 8 residues did not significantly affect the structural, Zn²⁺/DNA binding and catalytic properties of the protein [20]. The predicted pI value decreased by 0.08 units compared to the KGNK protein lacking these amino acids.

2. Results and Discussion

2.1. Structural Aspects of the Interaction of the KGNK Protein with Metal Ions as Observed via Circular Dichroism Spectroscopy

The interaction of the KGNK protein with various transition metal ions was monitored via circular dichroism (CD) spectroscopy in aqueous solutions. The selected metal ions were Zn²⁺ ion as a common catalytic metal ion in the hydrolytic enzymes, Ni²⁺ ion as the most common component of the immobilised metal ion affinity chromatography (IMAC) technique for protein purification, Cu²⁺ ion as a strong Lewis acid which could strongly compete for histidine side-chains with Zn²⁺ ions and Cd²⁺ ion as a d¹⁰ electron system analogue of Zn²⁺ ion.

The KGNK protein was purified via its glutathione-S-transferase (GST) fused form in the presence of the immunity protein Im7, as described earlier [20]. After the cleavage of the GST affinity tag, the resulting protein has a single strong metal ion binding site in the active centre. There is a remaining short amino acid sequence consisting of eight residues at the N-terminus of the protein after the cleavage. These residues do not affect the structure, the Zn²⁺ ion/DNA binding or the catalytic activity of the enzyme [20]. The Im7 protein was removed by decreasing the pH to 3.0 and separating the components using ion exchange chromatography. Under such conditions, the metal ion, originally bound to the enzyme during the expression, is also lost, likely due to both the structural changes in NCoIE7 and the competition of protons with the metal ion for the imidazole donor groups of histidines. The following buffer exchange to 20 mM HEPES (pH 7.7) recovered the functional structure of the protein. Thus, we expected to obtain the apoprotein as the product of this procedure. A fraction of the KGNK protein was incubated with 10 equivalents of EDTA, followed by a buffer exchange to 20 mM HEPES (pH 7.7) to remove the chelator. The CD spectra of enzyme before and after the above EDTA treatment were identical (Figure 2a), suggesting that the resulting protein was indeed the apoenzyme.

Previously, we have shown that the binding of Zn²⁺ ion to the apoenzyme causes a slight but significant change in the circular dichroism spectrum, reflected in a red shift of about 2 nm and accompanied by a small change in the intensity [20,24]. This change could be reproduced in the presence of one equivalent Zn²⁺ ion, while the addition of further Zn²⁺ ions did not affect the CD spectra (Figure 2b).

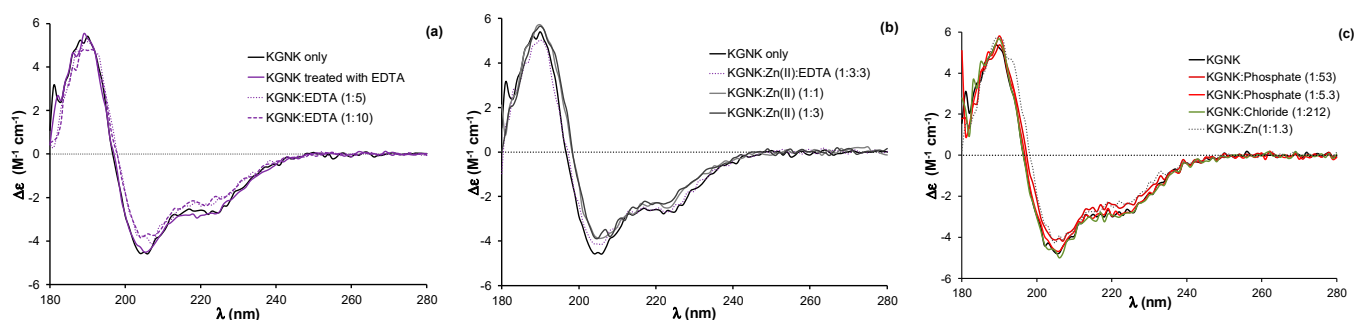


Figure 2. (a) Circular dichroism spectra of the KGNK protein with and without an additional treatment with EDTA and buffer exchange removing the chelator, and well as in the presence of increasing concentrations of EDTA. (b) Circular dichroism spectra of KGNK in the presence of increasing concentrations of Zn^{2+} ions, as well as the recovery of the apoenzyme via EDTA (dotted line). (c) The effect of simple (Cl^{-}) or complex (HPO_4^{2-}) anions on the KGNK CD spectral shape. The Zn^{2+} adduct is shown here for comparison. $\Delta\epsilon$ values are related to the amino acid residues.

The addition of equivalent non-endogenous metal ions, such as Ni^{2+} , Cu^{2+} or Cd^{2+} ions, to the apoprotein caused very similar changes in the CD spectra to those related to the effect of Zn^{2+} ion (Figure 3). The red shift of about 2 nm was observed independent of the applied metal ion concentration; the same changes were detected upon adding both one and three equivalents (compared to the protein) of metal ions. These changes reflect that all of the added metal ions could strongly bind to the KGNK active centre under the applied conditions, causing a minor change in the secondary structure of the protein. This might be surprising, since the structure of the HNH motif offers a preformed tetrahedral binding site, consisting of three histidines, which is optimal for Zn^{2+} -ions. At the same time, Ni^{2+} ions usually favour octahedral geometry, while Cu^{2+} would favour square planar coordination geometry. Nevertheless, Ni^{2+} ions were shown to bind to the HNH motif with a K_d of $\sim 1 \mu M$ [27]. The metal ion coordination could be reversed by the addition of EDTA in equivalent amounts compared to the metal ions in each case, yielding CD spectra identical to those of the apoenzyme.

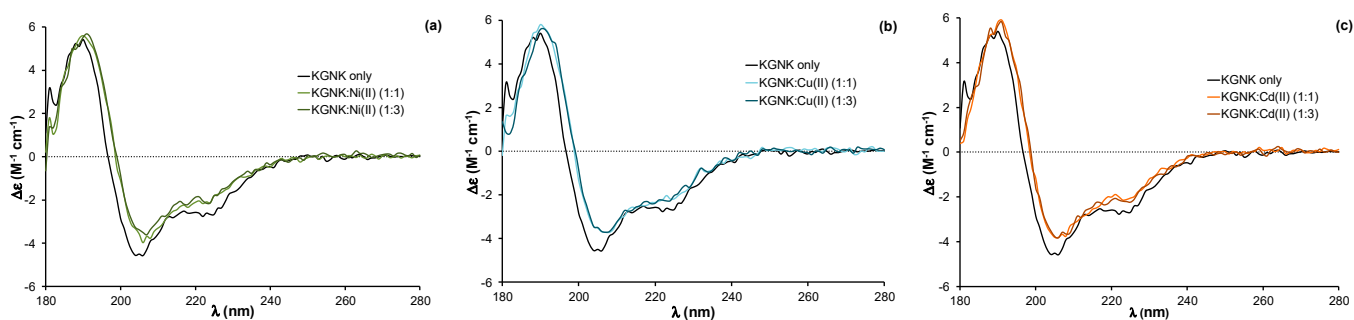


Figure 3. Circular dichroism spectra of the KGNK protein in the presence of increasing concentrations of (a) Ni^{2+} ions, (b) Cu^{2+} ions and (c) Cd^{2+} ions. $\Delta\epsilon$ values are related to the amino acid residues.

It is worthwhile to mention that the addition of excess EDTA to the apoenzyme (Figure 2a) caused a similar red shift of the spectra to that of the metal ions. This might be attributed to the interaction between the negatively charged EDTA with the positively charged residues of the protein otherwise participating in the DNA binding. The interaction with anions was already demonstrated by the crystal structure of an NCoLE7 mutant, in which phosphate ions occupied the positively charged DNA binding sites [16]. An excess of phosphate ions can also cause a slight change in the CD spectrum of the apo-KGNK, unlike the large excess of chloride ions (Figure 2c). Inhibition by the immunity protein Im7 is also largely based on similar interactions between the acidic side-chains of Im7 and basic side-chains of NCoLE7 [14]. Nevertheless, these results demonstrate that the

interaction with complex anions is not exclusively ionic, but also partially structural, e.g., hydrogen bonding.

2.2. Mass Spectrometric Monitoring of Metal Ion Binding to KGNK

The interaction of KGNK with metal ions was also investigated via mass spectrometry. Two main peaks were detected upon measuring the KGNK protein without the addition of metal ions: one with ~20% relative intensity related to that of the mono-metallated KGNK with Zn(II) and one with ~80% relative intensity assigned to the apoenzyme. Na⁺ and K⁺ adducts were also detected in the MS measurements (Figure 4a). This result suggested that apoenzyme at the applied low concentrations could easily acquire metal ions from buffers/reagents/containers/sample holders applied during the experiments, even if these were treated very carefully. The expected masses in comparison with the obtained ones are collected in Table 1.

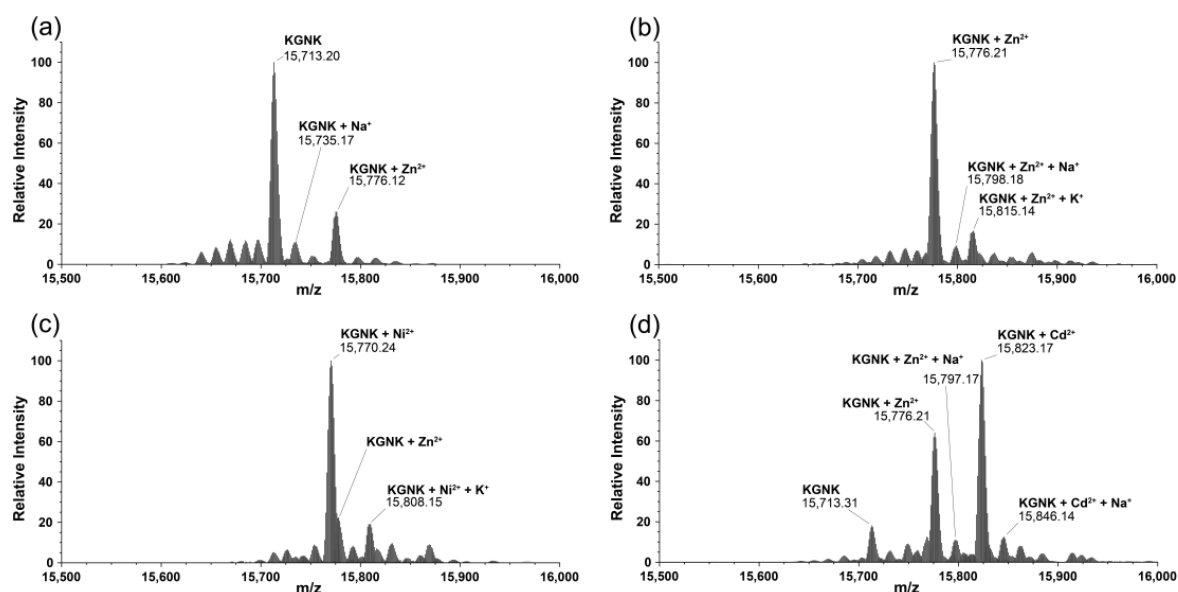


Figure 4. Deconvoluted ESI-MS spectra of the (a) KGNK protein; (b) KGNK + 1 eq Zn²⁺; (c) KGNK + 1 eq Ni²⁺ and (d) KGNK + 1 eq Cd²⁺; c_{KGNK} = 3.0 μM.

Table 1. Measured and calculated most abundant MH⁺ peaks of KGNK and its metal complexes.

Species	Formula	Calculated Mass of MH ⁺ (Da)	Measured Mass of MH ⁺ (Da)
KGNK apo	C ₆₉₀ H ₁₁₀₁ N ₂₁₁ O ₂₀₆ S ₂	15,713.19	15,713.20
KGNK + 1Zn ²⁺ −2H ⁺	C ₆₉₀ H ₁₀₉₉ N ₂₁₁ O ₂₀₆ S ₂ Zn	15,776.10	15,776.12
KGNK + 1Ni ²⁺ −2H ⁺	C ₆₉₀ H ₁₀₉₉ N ₂₁₁ O ₂₀₆ S ₂ Ni	15,770.11	15,770.24
KGNK + 1Cu ²⁺ −2H ⁺	C ₆₉₀ H ₁₀₉₉ N ₂₁₁ O ₂₀₆ S ₂ Cu	15,774.10	15,774.23
KGNK + 1Cd ²⁺ −2H ⁺	C ₆₉₀ H ₁₀₉₉ N ₂₁₁ O ₂₀₆ S ₂ Cd	15,823.08	15,823.17

Next, equivalent metal ions were added to the protein solution. It was observed that the apo KGNK coordinated the added Zn²⁺ ions, as well as the non-endogenous metal ions (Ni²⁺ and Cd²⁺) in the active centre. This resulted in the corresponding mono-metallated enzyme species according to the mass spectra in Figure 4b–d. In addition, at a molar ratio of 1:1, there was a small peak related to the Zn²⁺-bound KGNK protein.

This means that Ni²⁺ ions could bind to the apoprotein, but they could not replace the Zn²⁺ ions in the minor Zn²⁺-KGNK species. The formation of ternary complexes, including two different metal ions bound to the protein, could not be unequivocally excluded. The relative intensities of these peaks, to which the masses of such complexes could be assigned, were lower than 10%, and therefore their assignment was uncertain. Cd²⁺ ions proved to be

weaker interacting agents than Ni^{2+} ions, since one equivalent of Cd^{2+} ions could not even saturate the available apoprotein fully, so that a small peak related to the uncomplexed KGNK was still detected after the addition of one equivalent of this metal ion.

Most probably, the Cu^{2+} -bound protein was obtained upon the addition of equivalent Cu^{2+} ions (Figure 5). However, it was rather difficult to unequivocally prove the Cu^{2+} binding to KGNK via MS because of the small difference in the atomic weight, and as a consequence, in the molecular weight. For this reason, the isotope distribution pattern of the most abundant peak of the deconvoluted MH^+ mass spectrum at 15,774 m/z was compared with the simulated isotope pattern of the Cu^{2+} -KGNK and Zn^{2+} -KGNK complexes. The observed pattern of the recorded spectrum aligned well with the expected pattern of the Cu^{2+} complex. Therefore, it can be concluded that Cu^{2+} can bind to the protein, in accordance with the CD results.

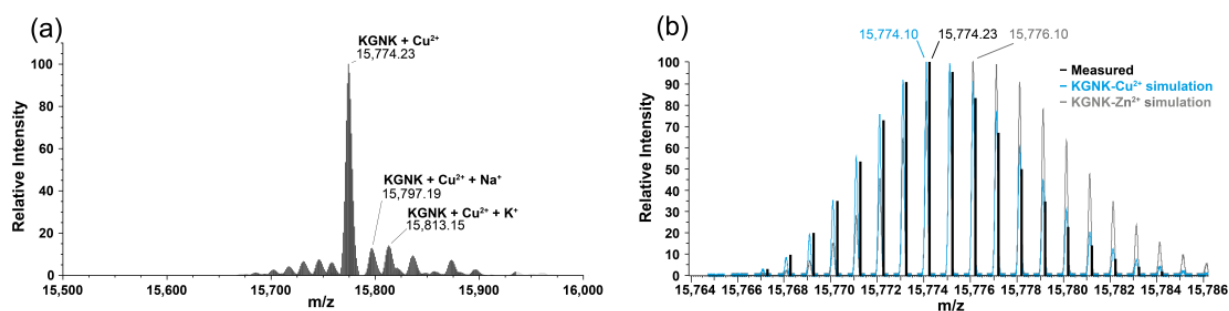


Figure 5. Deconvoluted ESI-MS spectra of (a) KGNK protein + 1 eq Cu^{2+} ; (b) comparison of the most abundant MH^+ peak of the ESI-MS spectra with the simulated spectra of Cu^{2+} -KGNK and Zn^{2+} -KGNK; $c_{\text{KGNK}} = 3.0 \mu\text{M}$.

We also observed a drastic change in the charge distribution pattern in the mass spectra as a consequence of the addition of the metal salt solutions (Figure 6). The apoprotein possessed a wide range of charged species, with two intensity maxima at $z = 16$ and 10 positive charges.

A similar phenomenon was previously published with NCoIE2, E7, E8 and E9 proteins, which are closely related bacterial toxins, upon Zn^{2+} binding at $\text{pH} = 7.2$. It was suggested that the apoprotein may exist in two different conformations, where one is an open structure and the other is a more stable one [28,29]. The latter is stabilised in the presence of the Zn^{2+} ion. As Figure 6 shows, all of the added metal ions could shift the charge distribution toward the structure exhibiting lower charges.

To verify the ability of the applied metal ions to compete with Zn^{2+} ions for the HNH motif in NCoIE7, one equivalent of the Zn^{2+} ions was added to the protein before supplementing the non-endogenous metal ions.

Upon the addition of one equivalent of Ni^{2+} , Cu^{2+} or Cd^{2+} ions to the Zn^{2+} -protein complex, the peak of the Zn^{2+} -bound protein was identified in each spectrum (Figure 7). Thus, none of the applied metal ions could compete with Zn^{2+} ions at a molar ratio of 1:1. This is in agreement with the fact that Zn^{2+} has a high affinity with the HNH motif, with K_d in the low nM range, as was suggested via the isothermal calorimetric titrations with NCoIE9 having an analogue HNH motif to NCoIE7 [27], as well as via similar investigations with NCoIE7 [20].

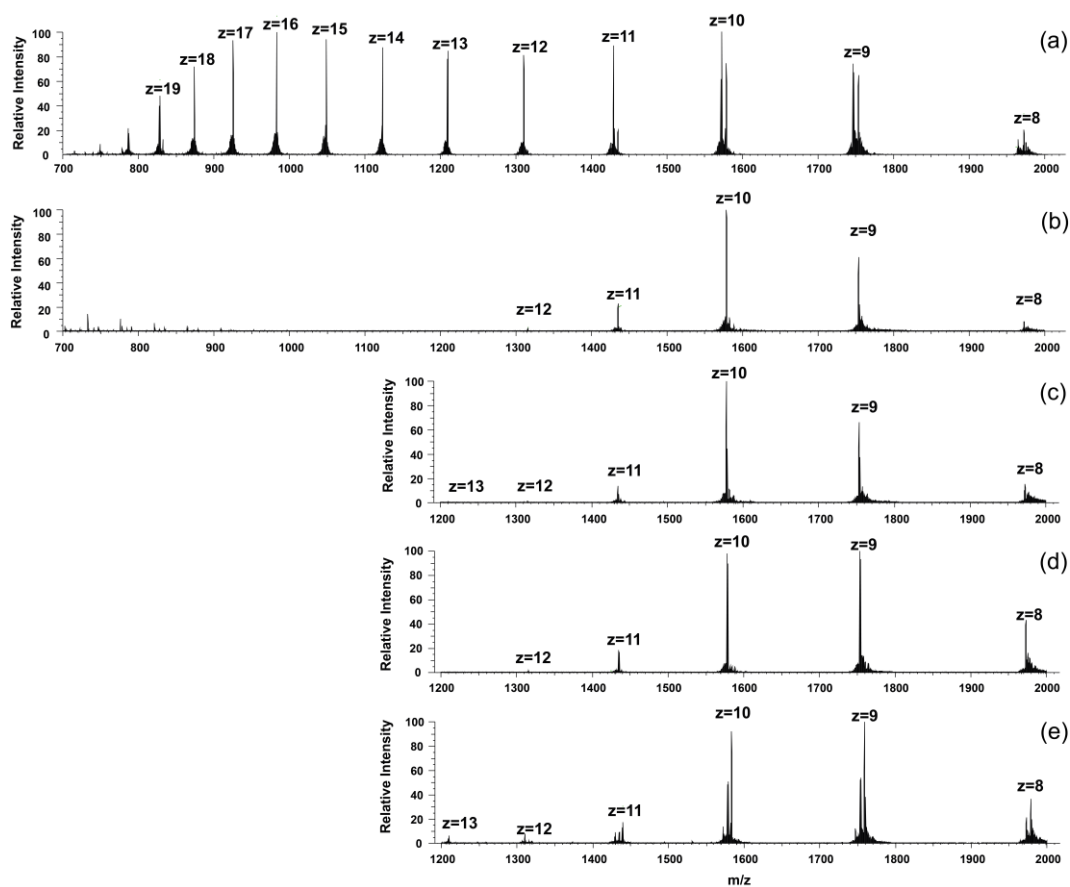


Figure 6. The recorded ESI-MS spectra of (a) KGNK protein; (b) KGNK + 1 eq Zn²⁺; (c) KGNK + 1 eq Ni²⁺; (d) KGNK + 1 eq Cu²⁺ and (e) KGNK + 1 eq Cd²⁺. $c_{\text{KGNK}} = 3 \mu\text{M}$.

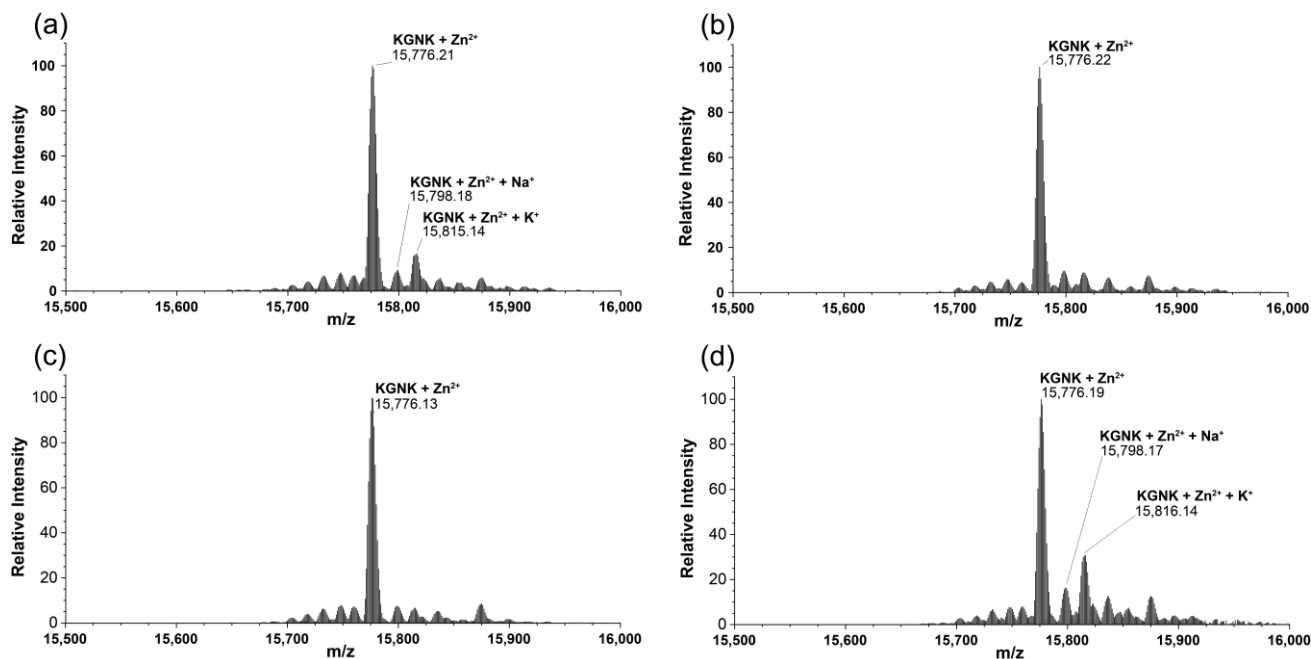


Figure 7. Deconvoluted ESI-MS spectra of KGNK protein in the presence of (a) 1 eq Zn²⁺; (b) 1 eq Zn²⁺ + 1 eq Cu²⁺; (c) 1 eq Zn²⁺ + 1 eq Ni²⁺ and (d) 1 eq Zn²⁺ + 1 eq Cd²⁺; $c_{\text{KGNK}} = 3.0 \mu\text{M}$.

2.3. The Effect of Metal Ions on the Catalytic Activity of KGNK

The nuclease activity of KGNK was studied using pUC119 plasmid DNA as a substrate via agarose gel electrophoresis. Starting with a DNA substrate mainly containing the superhelical form of the plasmid, first, the open circular form appears as a consequence of single-strand nicks. Then, linear DNA is formed upon double-strand cleavage. This would be preferred over the open circular form in the case of dimerisation of the enzyme upon DNA binding. Finally, a series of non-specific cleavages of DNA results in the distribution of DNA fragments (manifested as a smear) shifting to smaller and smaller sizes with time. Figure 8a shows that the enzyme was able to cleave the DNA efficiently, even without adding the metal ion to it. The mass spectrometric measurements already demonstrated that the apoenzyme solution may contain some Zn^{2+} ions acquired from the trace amounts of this metal ion in the environment (buffers/reactants/containers, etc.). The DNA solution may also contain a residual concentration of Zn^{2+} ions. However, the amount of Zn^{2+} -bound KGNK formed under these conditions should not cause a significant DNA cleavage. Previously, we have shown that the Zn^{2+} -bound KGNK mutant has moderate activity against plasmid DNA [20]. This was also indicated by the addition of one equivalent of Zn^{2+} ions, resulting in a less active enzyme compared to the “apo” form. This would surprisingly suggest that the metal ion that allows for this significant nuclease activity is different from Zn^{2+} , and it could not be detected via MS in such a small concentration. Interestingly, this activity could only slightly be inhibited by the addition of EDTA at up to 10 equivalents to the enzyme (results not shown). We suggest that the reason for this might be the competition between the positively charged amino acid side-chains for the negatively charged EDTA, as the interaction between EDTA and apo KGNK was already detected via CD spectroscopy (see above). Nevertheless, a large excess ($>10\times$) of EDTA can inhibit the enzyme.

The Zn^{2+} ions added at three equivalents caused slight inhibition of the enzymatic process. Although Zn^{2+} ions were suggested to be essential for the nuclease activity of NCoE7 [14,21], the excess of this metal ion was shown to have an inhibitory effect [21]. This might be attributed to the ability of the excess metal ion to prevent the H545-mediated OH^- generation via weak coordination to this histidine. Supplementing one equivalent of Cu^{2+} ions to the KGNK protein in the experiments, we observed similar behaviour to that of Zn^{2+} ions (Figure 8b). It is difficult to decide at this point whether the resulting low catalytic activity is due to the Cu^{2+} -bound enzyme, or whether it is due to the remnant activity of the apoenzyme after the partial replacement of the supposed unknown metal ion. Nevertheless, the excess of Cu^{2+} ions further decreased the catalytic activity that could best be observed at 2 h incubation.

More efficient DNA cleavage is observed in the presence of Cd^{2+} ions than with Zn^{2+} or Cu^{2+} ions (Figure 8c). However, this activity is still less than that of the control experiment with the KGNK protein in the absence of added metal ions. Furthermore, the activity is further decreased with increasing amounts of Cd^{2+} ions. This is in agreement with the mass spectrometric findings about the weak binding of Cd^{2+} ions to the KGNK enzyme.

The catalytic experiments in the presence of Ni^{2+} ions demonstrated much higher activity with this metal ion than the apoprotein used as a control (Figure 8d vs. Figure 8a). It is even more intriguing that the excess of the Ni^{2+} ions did not significantly inhibit this highly active enzyme. The comparison of the time dependence of the band intensity related to the superhelical DNA form is shown in Figure 8e. These data indicate that although Zn^{2+} is more strongly bound to the KGNK protein than the other divalent metal ions by at least three orders of magnitude [27], and thus Ni^{2+} may not be the native metal ion, its presence still results in high activity of the enzyme. This suggests that Ni^{2+} ions promote the DNA cleavage of the enzyme via different mechanisms than those of the Zn^{2+} -bound KGNK. While the nucleophilic OH^- ion generation mediated by H545 is not so efficient in this mutant than in NCoE7, the Ni^{2+} ion may promote the deprotonation of a coordinated water molecule, which can serve as an attacking agent for DNA hydrolysis. The crystal structure of NCoE7 with Ni^{2+} ion supports this assumption, showing that the metal ion is

coordinated to a phosphate ion and a water molecule besides the three histidine side-chains in distorted trigonal bi-pyramidal geometry [17].

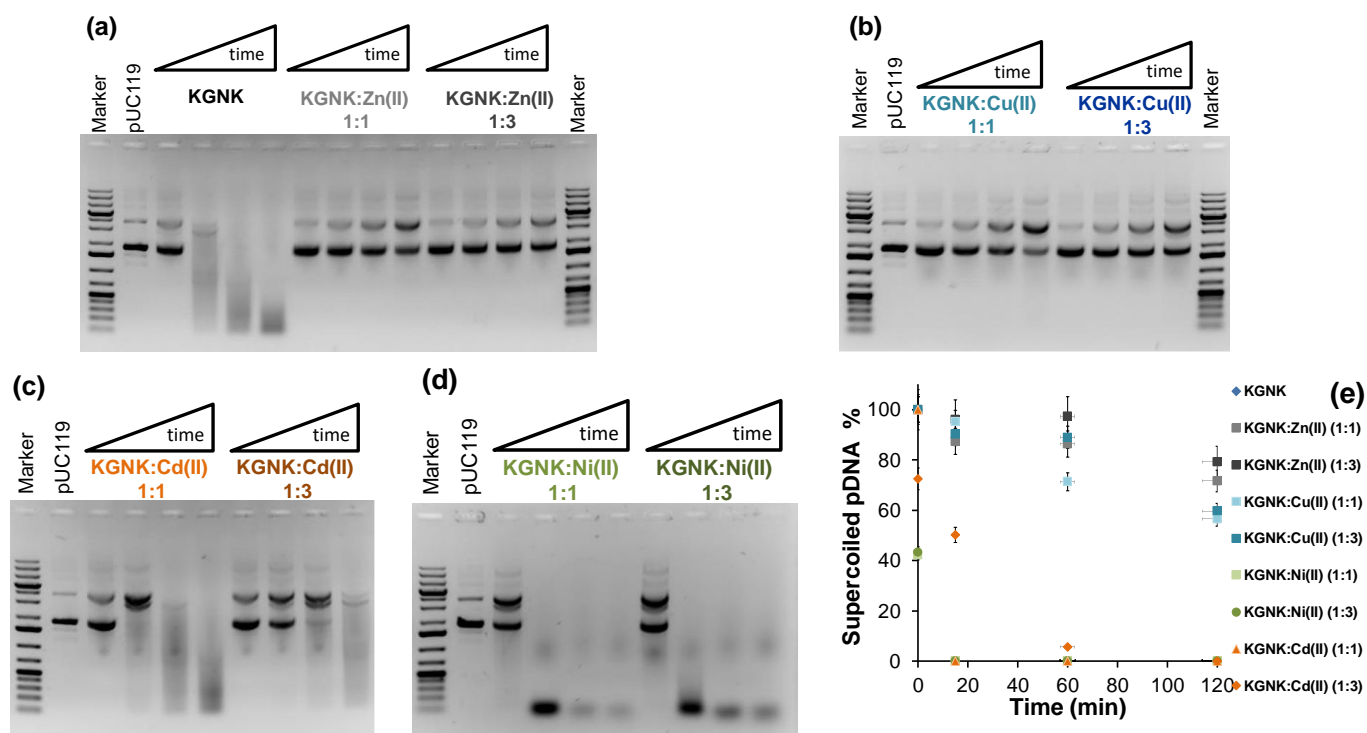


Figure 8. Detection of the pUC119 plasmid DNA ($c = 74 \mu\text{M}$ for base pairs (bp), 3162 bp) cleavage by $1 \mu\text{M}$ KGNK enzyme using 1% (w/v) agarose gel electrophoresis in the absence and presence of various metal ions. The results with the apoenzyme and metallised KGNK with Zn^{2+} ions (a), and the apoenzyme in the presence of Cu^{2+} ions (b), Ni^{2+} ions (c) and Cd^{2+} ions (d) at 1:1 or 1:3 KGNK/metal ion molar ratios, respectively. Each well of the agarose gel in a cleavage experiment represents the catalytic activity after 0, 15, 60, or 120 min, from left to right. Gene Ruler 1 kb plus DNA Ladder (Thermo Scientific, Vilnius, Lithuania) was applied as a reference, and pUC119 ($c = 74 \mu\text{M}$ for base pairs) as a negative control was loaded on the gels. (e) The time dependence of the intensity of the band related to the superhelical form of the plasmid DNA in the absence and presence of various metal ions.

To verify that the DNA cleavage was induced by Ni^{2+} ions bound in the active site of the enzyme, we carried out competition experiments with Zn^{2+} ion. Independent of the order of addition of each component of the mixture, i.e., first adding Zn^{2+} and then Ni^{2+} , or in the reverse order, identical observations were made (Figure 9a).

Accordingly, the catalytic activity substantially decreased in comparison to that of the Ni^{2+} -bound enzyme. This is rather characteristic of the Zn^{2+} -enzyme complex. This reflects the replacement of the Ni^{2+} ions by the Zn^{2+} ions due to the thermodynamics, i.e., due to the stronger binding of Zn^{2+} ions to the active centre. This is in accordance with the results from the mass spectrometric experiments carried out under competitive conditions. Figure 9b shows that Ni^{2+} ions cannot initiate DNA cleavage in the absence of the enzyme under the applied conditions. From these results, we can conclude that the R447G-modified NCoIE7 protein prefers to bind Zn^{2+} ion in its active centre, but it has much higher activity in its Ni^{2+} form, providing a chance for enzymatic regulation by the metal ion environment.

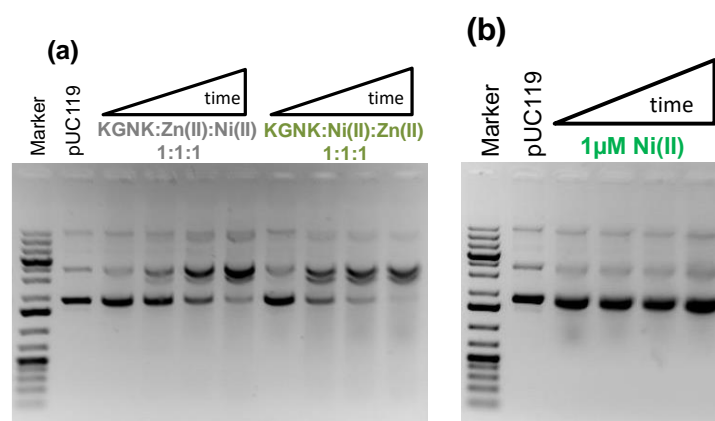


Figure 9. Detection of the pUC119 plasmid DNA ($c = 74 \mu\text{M}$ for bp, 3162 bp) cleavage using 1% (w/v) agarose gel electrophoresis. (a) $1 \mu\text{M}$ KGNK enzyme was applied under metal ion competition conditions, either supplementing Zn^{2+} first and then Ni^{2+} in the reaction mixture or in the opposite order. (b) Interaction of DNA with Ni^{2+} at $1 \mu\text{M}$ as a control experiment. Each well of the agarose gel in a cleavage experiment represents the catalytic activity after 0, 15, 60, or 120 min, from left to right. Gene Ruler 1 kb plus DNA Ladder (Thermo Scientific) was applied as a reference, and pUC119 ($c = 74 \mu\text{M}$ for base pairs) was loaded on the gels as a negative control.

3. Materials and Methods

3.1. Reagents

All of the reagents were used as purchased, without further purification. Seakem LE agarose was obtained from Lonza, Rockland, ME, USA and LB medium, ZnCl_2 , NiCl_2 , CdCl_2 , CuCl_2 , disodium-EDTA, Na_2HPO_4 and NaH_2PO_4 were obtained from Reanal Ltd, Budapest, Hungary. NaCl (Szkarabeusz Laboratory, Chemical Industry and Trade Ltd., Pecs, Hungary) was used, and Acrylamide/bis-acrylamide (29/1) as a 30% (w/v) solution was from SERVA Electrophoresis GmbH, Heidelberg, Germany and VWR Chemicals, LLC; Solon, Ohio, USA. Bisacrylamide 2K (standard grade, extra pure) was bought from AppliChem Panreac, Darmstadt, Germany. KCl and tris(hydroxymethyl)aminomethane were purchased from Molar Chemicals Ltd., Halásztelek, Hungary. N-2-hydroxyethylpiperazine-N-2-ethane sulfonic acid (HEPES) and ammonium bicarbonate were from Sigma-Aldrich, St. Louis, MO, USA, glycine was from Duchefa Biochemie B. V., Haarlem, The Netherlands, tricine and SDS were from VWR Chemicals and isopropyl β -D-1-thiogalactopyranoside (IPTG, dioxane-free) was obtained from Thermo Scientific, while ampicillin sodium salt was purchased from Sigma-Aldrich. The pGEX-6P-1 vector was a GE Healthcare Bio-Sci, Chicago, USA product. *Escherichia coli* (*E. coli*) DH10B F- end A1 recA1 galU galK deoR nupG rpsL Δ lacX74 Φ 80lacZ Δ M15 araD139 Δ (ara,leu)7697 mcrA Δ (mrr-hsdRMS-mcrBC) Δ - was applied for cloning [30], while *E. coli* BL21 (DE3) F- ompT gal [dcm] [lon] hsdSB was used for protein expression [31].

3.2. Recombinant NColE7-KGNK Expression and Purification

The construction of the pGEX-6P-1-KGNK vector with an inserted R447G mutant of the nuclease domain of colicin E7 (NColE7) and the KGNK protein expression and purification with N-terminal Glutathione-S-Transferase (GST) fusion were described previously [20]. After the purification, the GST tag was cleaved according to the described method in [20]. The buffer of the purified product was exchanged to 20 mM N-2-hydroxyethylpiperazine-N-2-ethane sulfonic acid (HEPES) pH 7.7 using an Amicon ultra 15 mL centrifugal filter (Merck Millipore Ltd., Tullagreen Carrigtwohill, Co Cork IRL, Ireland). The purification steps of the protein were monitored via 15% (w/v) sodium dodecyl sulphate polyacrylamide gel electrophoresis (SDS PAGE) using a mixture of 116, 66.2, 45, 35, 25, 18.4 and 14.4 kDa unstained proteins as a marker (Thermo Scientific #26610). The experiment was carried out at 70 V for 30 min and then 120 V for 150 min using 0.1 M Tris-HCl, 0.1 M tricine and

0.1% (*w/v*) SDS, pH 8.3 cathode and 0.2 M Tris-HCl, and pH 8.9 anode buffers at RT. The resulting single band approved the homogeneity of the purified protein. The concentration of the purified protein was checked using UV absorbance spectrometry, recording the absorbance at 280 nm against the buffer baseline (Cary 8454 UV-Vis spectrophotometer, Agilent Technologies, Santa Clara, CA, USA). The molar absorbance of the protein used for the calculation of the concentration was estimated using an Expasy ProtParam tool [32] to be $12,490 \text{ M}^{-1} \text{ cm}^{-1}$. The circular dichroism spectrum was identical to that measured for the previously used batches of the protein.

3.3. Mass Spectrometric Experiments

Intact protein analysis was performed on an LTQ-Orbitrap Elite (Thermo Scientific) mass spectrometer coupled with a TriVersa NanoMate (Advion, Ithaca, NY, USA) chip-based electrospray ion source. Measurements were carried out in positive mode at 120,000 resolution in 2.5 mM ammonium hydrogen carbonate buffer (pH ~7.8). The protein concentration was 3.0 μM in each individual sample which contained various metal ions (added as ZnCl_2 , CuCl_2 , NiCl_2 or CdCl_2) at different molar ratios. Data evaluation, deconvolution to yield the masses of MH^+ ions and spectrometric pattern simulations were performed using the Freestyle 1.6 or Xcalibur 2.2 software (Thermo Scientific). Analysing the data via the deconvolution of 10×10 consecutive scans we found that the standard deviation of the peak positions was less than 0.02 mass units. We did not make strict quantitative conclusions from the ESI MS spectra.

3.4. Circular Dichroism Spectroscopic Measurements

Circular dichroism (CD) spectra were recorded at room temperature utilising a Jasco J-1500 CD spectrometer using the following parameters. Wavelength range: 280–180 nm; path length: 0.2 mm (Jasco cuvette); D.I.T.: 2 s; bandwidth: 1.0 nm; scanning speed: 50 nm/min (continuous scanning mode); each spectrum was the average of three accumulated measurements. The concentration of the enzyme was 18.0 μM in 3–10 mM HEPES, pH 7.7. The measurements were carried out with apo enzyme, and in the presence of EDTA and/or various metal salts (ZnCl_2 , CuCl_2 , NiCl_2 and CdCl_2) at indicated molar ratios. Water and the buffer spectra were recorded for baseline correction, and the spectra were plotted without smoothing.

3.5. Catalytic Activity Assay

The catalytic activity of the KGNK mutant protein was monitored against plasmid DNA (pUC119) as a substrate. In a few experiments, the KGNK protein was treated with EDTA for comparison. The final concentration of the enzyme was 1.0 μM , while the DNA was 74 μM for base pairs in 20 mM HEPES, pH 7.7. The DNA cleavage was performed in the absence and presence of different metal ions of Zn^{2+} , Cu^{2+} , Cd^{2+} and Ni^{2+} , at molar ratios of the enzyme to metal ion (1:1 and 1:3). The reaction mixtures were prepared by mixing all of the components, except for the plasmid DNA (pUC119) which was added to the mixture last. Then, it was incubated at 37 °C for various periods. Aliquots of 5 μL of the reaction mixture were taken four times and the reaction was stopped by adding 5 μL of 2% (*w/v*) SDS solution (1% (*w/v*) at final concentration) for enzyme denaturation. At least three replicates were carried out for each experiment.

The products of the DNA cleavage assays were checked via agarose gel electrophoresis (AGE). The products were run in 1% (*w/v*) agarose gel containing 0.5 $\mu\text{g/mL}$ ethidium bromide for the visualisation of the DNA. Electrophoresis was performed in the TAE buffer (40 mM tris(hydroxymethyl) aminomethane, 20 mM acetic acid and 1 mM ethylenediaminetetraacetic acid, pH 8.0) using Bio-Rad wide mini sub cell VR GT, applying 7 V/cm potential gradients (100 V for 40 min). Gene Ruler 1 kb Plus DNA Ladder (Thermo Scientific) served as the reference, and non-cleaved plasmid DNA (pUC119) as a negative control was applied for comparison.

4. Conclusions

The R447G mutant of the nuclease domain of colicin E7 bacterial toxin was studied in this project in the presence of non-endogenous metal ions such as Ni²⁺, Cu²⁺ and Cd²⁺. The mutated protein with decreased activity allowed for easier monitoring of the catalytic process, but it also may have offered a new mechanism for DNA cleavage, since it lacks an important residue participating in DNA cleavage. This seems to be an intriguing question to answer.

Our circular dichroism and mass spectrometric results revealed that all of the metal ions used in this study bound to the active centre of the enzyme in the absence of Zn²⁺. However, they could not replace Zn²⁺ if it was already present in the active site. It was detected that the enzyme is very active in the presence of substoichiometric metal ion, which is difficult to remove via EDTA because of the competitive behaviour of the positively charged amino acid side-chains of the protein. It is also not unprecedented that a nuclease enzyme cleaves DNA in the absence of metal ions such as BfiI type II restriction endonuclease or the EDTA-resistant nuclease Nuc of *Salmonella typhimurium* [33,34]. On the other hand, we could see very high activity of the enzyme in the presence of Ni²⁺ ions, which could not be inhibited by the excess of the metal ion, but it was considerably inhibited by Zn²⁺, independent of the order of the metal ions added. These results suggest that the R447G enzyme cleaves DNA in a different manner from that of NCoIE7. We aim to deal with this exciting problem in a future project.

Author Contributions: Conceptualisation, B.G.; investigation, Z.H.N., B.H. and É.H.-G.; data curation, É.H.-G. and B.G.; writing—original draft preparation, Z.H.N. and B.G.; writing—review and editing, Z.H.N., B.H., É.H.-G. and B.G.; funding acquisition, É.H.-G. and B.G. All authors have read and agreed to the published version of the manuscript.

Funding: This research was funded and supported by the Hungarian National Research, Development and Innovation Office (grant numbers: GINOP-2.3.2-15-2016-00038, GINOP-2.3.2-15-2016-00001, GINOP-2.3.2-15-2016-00020, 2019-2.1111-TÉT-2019-00089 and K_16/120130).

Institutional Review Board Statement: Not applicable.

Informed Consent Statement: Not applicable.

Data Availability Statement: Not applicable.

Acknowledgments: The authors thank Eszter Németh for providing advice on KGNK protein purification.

Conflicts of Interest: The authors declare no conflict of interest. The funders had no role in the design of the study; in the collection, analyses or interpretation of data; in the writing of the manuscript or in the decision to publish the results.

Sample Availability: Samples of the DNA vectors are available from the authors.

References

1. Klein, A.; Wojdyla, J.A.; Joshi, A.; Josts, I.; McCaughey, L.C.; Housden, N.G.; Kaminska, R.; Byron, O.; Walker, D.; Kleanthous, C. Structural and biophysical analysis of nuclease protein antibiotics. *Biochem. J.* **2016**, *473*, 2799–2812. [[CrossRef](#)]
2. Marković, K.G.; Grujović, M.Ž.; Koraćević, M.G.; Nikodijević, D.D.; Milutinović, M.G.; Semedo-Lemsaddek, T.; Djilas, M.D. Colicins and Microcins Produced by Enterobacteriaceae: Characterization, Mode of Action, and Putative Applications. *Int. J. Environ. Res. Public Health* **2022**, *19*, 11825. [[CrossRef](#)]
3. Cascales, E.; Buchanan, S.K.; Duche, D.; Kleanthous, C.; Lloubes, R.; Postle, K.; Riley, M.; Slatin, S.; Cavard, D. Colicin Biology. *Microbiol. Mol. Biol. Rev.* **2007**, *71*, 158–229. [[CrossRef](#)]
4. Papadakos, G.; Wojdyla, J.A.; Kleanthous, C. Nuclease colicins and their immunity proteins. *Q. Rev. Biophys.* **2012**, *45*, 57–103. [[CrossRef](#)] [[PubMed](#)]
5. Chak, K.F.; Kuo, W.S.; Lu, F.M.; James, R. Cloning and characterization of the ColE7 plasmid. *J. Gen. Microbiol.* **1991**, *137*, 91–100. [[CrossRef](#)] [[PubMed](#)]
6. Hsia, K.C.; Li, C.-L.; Yuan, H.S. Structural and functional insight into sugar-nonspecific nucleases in host defense. *Curr. Opin. Struct. Biol.* **2005**, *15*, 126–134. [[CrossRef](#)] [[PubMed](#)]

7. Liao, C.C.; Hsiao, K.C.; Liu, Y.W.; Leng, P.H.; Yuen, H.S.; Chak, K.-F. Processing of DNase domain during translocation of colicin E7 across the membrane of *Escherichia coli*. *Biochem. Biophys. Res. Commun.* **2001**, *284*, 556–562. [[CrossRef](#)]
8. Hsia, K.C.; Chak, K.F.; Liang, P.H.; Cheng, Y.S.; Ku, W.Y.; Yuan, H.S. Crystal structures of nuclease-Cole7 complexed with octamer DNA. *Structure* **2004**, *12*, 205–214. [[CrossRef](#)] [[PubMed](#)]
9. Mora, L.; de Zamaroczy, M. In Vivo Processing of DNase Colicins E2 and E7 Is Required for Their Import into the Cytoplasm of Target Cells. *PLoS ONE* **2014**, *9*, e96549. [[CrossRef](#)]
10. Cheng, Y.S.; Hsia, K.C.; Doudeva, L.G.; Chak, K.F.; Yuan, H.S. The crystal structure of the nuclease domain of colicin E7 suggests a mechanism for binding to double-stranded DNA by the H-N-H endonucleases. *J. Mol. Biol.* **2002**, *324*, 227–236.
11. Eastberg, J.H.; Eklund, J. Mutability of an HNH Nuclease Imidazole General Base and Exchange of a Deprotonation Mechanism. *Biochemistry* **2007**, *46*, 7215–7225. [[CrossRef](#)] [[PubMed](#)]
12. Huang, H.; Yuan, H.S. The Conserved Asparagine in the HNH Motif Serves an Important Structural Role in Metal Finger Endonucleases. *J. Mol. Biol.* **2007**, *368*, 812–821. [[CrossRef](#)] [[PubMed](#)]
13. Levin, K.B.; Dym, O.; Albeck, S.; Magdassi, S.; Keeble, A.H.; Kleanthous, C.; Tawfik, D.S. Following evolutionary paths to protein-protein interactions with high affinity and selectivity. *Nat. Struct. Mol. Biol.* **2009**, *16*, 1049–1055. [[CrossRef](#)] [[PubMed](#)]
14. Ko, T.; Liao, C.; Ku, W.; Chak, K.; Yuan, H.S. The crystal structure of the DNase domain of colicin E7 in complex with its inhibitor Im7 protein. *Structure* **1999**, *7*, 91–102. [[CrossRef](#)]
15. Sui, M.; Tsai, L.; Hsia, K.; Doudeva, L.; Ku, W.; Han, G.; Yuan, H. Metal ions and phosphate binding in the H-N-H motif: Crystal structures of the nuclease domain of Cole7/Im7 in complex with a phosphate ion and different divalent metal ions. *Protein Sci.* **2002**, *11*, 2947–2957. [[CrossRef](#)]
16. Czene, A.; Tóth, E.; Németh, E.; Otten, H.; Poulsen, J.N.; Christensen, H.E.M.; Rulišek, L.; Nagata, K.; Larsen, S.; Gyurcsik, B. A new insight into the zinc-dependent DNA-cleavage by the colicin E7 nuclease: A crystallographic and computational study. *Metallomics* **2014**, *6*, 2090–2099. [[CrossRef](#)]
17. Doudeva, L.; Huang, D.; Hsia, K.; Shi, Z.; Li, C.; Shen, Y.; Cheng, Y.; Yuan, H. Crystal structural analysis and metal-dependent stability and activity studies of the Cole7 endonuclease domain in complex with DNA/Zn²⁺ or inhibitor/Ni²⁺. *Protein Sci.* **2006**, *15*, 269–280.
18. Wang, Y.; Yang, W.; Li, C.; Doudeva, L.G.; Yuan, H.S. Structural basis for sequence-dependent DNA cleavage by nonspecific endonucleases. *Nucleic Acids Res.* **2007**, *35*, 584–594. [[CrossRef](#)]
19. Czene, A.; Németh, E.; Zóka, I.G.; Jakab-Simon, N.I.; Körtvélyesi, T.; Nagata, K.; Christensen, H.E.M.; Gyurcsik, B. The role of the N-terminal loop in the function of the colicin E7 nuclease domain. *J. Biol. Inorg. Chem.* **2013**, *18*, 309–321.
20. Németh, E.; Körtvélyesi, T.; Thulstrup, P.W.; Christensen, H.E.M.; Kožíšek, M.; Nagata, K.; Czene, A.; Gyurcsik, B. Fine tuning of the catalytic activity of colicin E7 nuclease domain by systematic N-terminal mutations. *Protein Sci.* **2014**, *23*, 1113–1122. [[CrossRef](#)]
21. Ku, W.; Liu, Y.; Hsu, Y.; Liao, C.; Liang, P.; Yuan, H.; Chak, K. The zinc ion in the HNH motif of the endonuclease domain of colicin E7 is not required for DNA binding but is essential for DNA hydrolysis. *Nucleic Acids Res.* **2002**, *30*, 1670–1678. [[CrossRef](#)] [[PubMed](#)]
22. Németh, E.; Körtvélyesi, T.; Kožíšek, M.; Thulstrup, P.W.; Christensen, H.E.M.; Asaka, M.N.; Nagata, K.; Gyurcsik, B. Substrate binding activates the designed triple mutant of the colicin E7 metallonuclease. *J. Biol. Inorg. Chem.* **2014**, *19*, 12951303. [[CrossRef](#)] [[PubMed](#)]
23. Németh, E.; Kožíšek, M.; Schilli, G.K.; Gyurcsik, B. Preorganization of the catalytic Zn²⁺ binding site in the HNH nuclease motif-A solution study. *J. Inorg. Biochem.* **2015**, *151*, 143–149. [[CrossRef](#)] [[PubMed](#)]
24. Németh, E.; Balogh, R.K.; Borsos, K.; Czene, A.; Thulstrup, P.W.; Gyurcsik, B. Intrinsic protein disorder could be overlooked in cocrystallization conditions: An SRCO case study. *Protein Sci.* **2016**, *25*, 1977–1988. [[CrossRef](#)]
25. Shi, Z.; Chak, K.F.; Yuan, H.S. Identification of an essential cleavage site in Cole7 required for import and killing of cells. *J. Biol. Chem.* **2005**, *280*, 24663–24668. [[CrossRef](#)]
26. Shlyapnikov, S.V.; Lunin, V.V.; Perbandt, M.; Polyakov, K.M.; Lunin, V.Y.; Levnikov, V.M.; Betzel, C.; Mikhailov, A.M. Atomic structure of the *Serratia marcescens* endonuclease at 1.1 Å resolution and the enzyme reaction mechanism. *Acta Crystallogr. D Biol. Crystallogr.* **2000**, *56*, 567–572. [[CrossRef](#)]
27. Pommer, A.J.; Kuhlmann, U.C.; Cooper, A.; Hemmings, A.M.; Moore, G.R.; James, R.; Kleanthous, C. Homing in on the role of transition metals in the HNH motif of colicin endonuclease. *J. Biol. Chem.* **1999**, *274*, 27153–27160. [[CrossRef](#)]
28. van den Bremer, E.T.; Jiskoot, W.; James, R.; Moore, G.R.; Kleanthous, C.; Heck, A.J.; Maier, C.S. Probing metal ion binding and conformational properties of the colicin E9 endonuclease by electrospray ionization time-of-flight mass spectrometry. *Protein Sci.* **2002**, *11*, 1738–1752. [[CrossRef](#)]
29. van den Bremer, E.T.; Keeble, A.H.; Jiskoot, W.; Spelbrink, R.E.; Maier, C.S.; van Hoek, A.; Visser, A.J.; James, R.; Moore, G.R.; Kleanthous, C.; et al. Distinct conformational stability and functional activity of four highly homologous endonuclease colicins. *Protein Sci.* **2004**, *13*, 1391–1401. [[CrossRef](#)]
30. Grant, S.G.N.; Jessee, J.; Bloom, F.R.; Hanahan, D. Differential plasmid rescue from transgenic mouse DNAs into *Escherichia coli* methylation-restriction mutants. *Proc. Natl. Acad. Sci. USA* **1990**, *87*, 4645–4649. [[CrossRef](#)]
31. Studier, F.W.; Rosenberg, A.H.; Dunn, J.J.; Dubendorff, J.W. Use of T7 RNA polymerase to direct expression of cloned genes. *Methods Enzymol.* **1990**, *185*, 60–89. [[PubMed](#)]

32. Gasteiger, E.; Hoogland, C.; Gattiker, A.; Duvaud, S.; Wilkins, M.R.; Appel, R.D.; Bairoch, A. Protein identification and analysis tools on the ExPasy server. In *The Proteomics Protocols Handbook*; Walker, J.M., Ed.; Humana Press: Totowa, NJ, USA, 2005; pp. 571–607.
33. Lagunavicius, A.; Sasnauskas, G.; Halford, S.E.; Siksnys, V. The metal-independent type IIs restriction enzyme BfiI is a dimer that binds two DNA sites but has only one catalytic centre. *J. Mol. Biol.* **2003**, *326*, 1051–1064. [[CrossRef](#)] [[PubMed](#)]
34. Pohlman, R.F.; Liu, F.; Wang, L.; More, M.I.; Winans, S.C. Genetic and biochemical analysis of an endonuclease encoded by the IncN plasmid pKM101. *Nucleic Acids Res.* **1993**, *21*, 4867–4872. [[CrossRef](#)] [[PubMed](#)]

Disclaimer/Publisher’s Note: The statements, opinions and data contained in all publications are solely those of the individual author(s) and contributor(s) and not of MDPI and/or the editor(s). MDPI and/or the editor(s) disclaim responsibility for any injury to people or property resulting from any ideas, methods, instructions or products referred to in the content.